



Supplementary Information for

R-spondin substitutes for neuronal input for taste cell regeneration in adult mice

Xiaoli Lin¹, Chanyi Lu¹, Makoto Ohmoto¹, Katarzyna Choma¹, Robert F. Margolskee¹,
Ichiro Matsumoto¹, Peihua Jiang^{1*}

¹ Monell Chemical Senses Center, Philadelphia, PA 19104

*Corresponding author: Peihua Jiang

Email: pjiang@monell.org

This PDF file includes:

Supplementary text
Figures S1 to S9

Supplementary Information Text
Materials and Methods:

Nerve transection and viral infection: For glossopharyngeal nerve (GL) transection, 7- to 10-week-old mice (wild-type and $Lgr5^{EGFP-IRES-CreERT2+/-}; Rosa26^{tdTomato}$) were deeply anesthetized with continuous flow of 2% isoflurane and placed on isothermal heating pads. We followed a procedure described previously to bilaterally transect the GL (1). Briefly, mice were placed in a supine position. We made an incision along the ventral neck midline, the digastric muscle was retracted to expose the GL, bilateral transection was performed, and the incision was closed with sutures. Sham-operated mice received the same procedure with exception of transection of the GL. All experiments were performed under National Institutes of Health *Guidelines for the Care and Use of Animals in Research* and approved by the Institutional Animal Care and Use Committee of the Monell Chemical Senses Center (protocol # 1150).

At day 4 postoperation, some mice received a single tail vein injection of Ad-Rspo1-Fc or Ad-Fc (control adenovirus) at 3×10^8 pfu per mouse, or Ad-Rspo2-Fc or Ad-Fc at 1×10^9 pfu per mouse. A single intraperitoneal tamoxifen injection (Sigma-Aldrich, T5648, 0.1 mg/g body weight in corn oil) was performed on GL-transected (GLx) $Lgr5^{EGFP-IRES-CreERT2+/-}; Rosa26^{tdTomato}$ mice at the time of virus infection for lineage tracing. Mice were euthanized 2 weeks after GLx or sham operation. Tissues such as tongue and gut were collected for histological and immunohistochemistry analyses.

Immunostaining and imaging: Immunostaining was performed essentially as described previously (2, 3). Briefly, tongues were fixed in 4% (wt/vol) paraformaldehyde for 2 h, cryoprotected with 30% sucrose overnight, and sectioned at 10 μ m. To identify taste

cells, we used specific primary antibodies against taste cell markers and species-specific secondary antibodies: goat anti-Car4 (R&D, 1:100, Cat. # AF2414, RRID: AB_2070332), rabbit anti-P2X3 (Alomone Labs, 1:1000, Cat. # APR-016, RRID: AB_2313760), rabbit anti-Plc β 2 (Santa Cruz, 1:500, Cat. # SC-206, RRID: AB_632197), and rat anti-Krt8 (Developmental Studies Hybridoma Bank, 1:10, Cat. # Troma-1, RRID: AB_531826). For sections from wild-type mice, double staining was performed, such as pairs of anti-Car4 and anti-P2X3 antibodies, and anti-Plc β 2 and anti-Krt8 antibodies. For sections from *Lgr5*^{EGFP-IRE5-CreERT2+/-}; *Rosa26*^{tdTomato} mice, single staining with anti-Krt8 or anti-P2X3 was performed. Fluorescence-labeled secondary antibodies (1:500) against specific species were used to visualize staining (donkey anti-goat Alexa Fluor 488, Abcam, Cat. # Ab150129, RRID: AB_2687506; donkey anti-rabbit Alexa Fluor 555, Abcam, Cat. # Ab150074, RRID: AB_2636997; donkey anti-rat Alexa Fluor 488, Molecular Probes, Cat. # A-21208, RRID: AB_2535794). For sections from *Lgr5*^{EGFP-IRE5-CreERT2+/-}; *Rosa26*^{tdTomato} mice, donkey anti-rabbit Alexa Fluor 647 (Abcam, Cat. # ab150075, RRID: AB_2752244) and donkey anti-rat Alexa Fluor 647 (Abcam, Cat. # ab150155, RRID: AB_2813835) were used. In addition, for initial characterization of the effect of nerve transection of wild-type mice (including 1 sham-operated, 2 GLx, and 2 GLx + Ad-Rspo1-Fc mice), we fixed tongues overnight prior to cryoprotection and sectioning and performed antigen retrieval (Agilent, S236784-2) prior to immunostaining, for better visualization of Plc β 2- and P2X3-immunoreactive signals. All images were acquired by a Leica TCS SP8 confocal microscope at the Cell and Developmental Biology Core at the University of Pennsylvania or a Nikon Eclipse E800

microscope. Confocal images were compressed z-stacks of the entire section (~10 μm); single optical sections gave rise to the same results as the z-stacks.

Cell profile counting: In each section on a slide, immunostained cells were counted by manually counting visible cell profiles (elongated cells with a clear nucleus) in taste epithelium along the lateral trench walls of the circumvallate papilla, taste bud cells on the dorsum of the papilla were not included in the counting. In images that had groups of overlapping cells, the cell profile count was conducted two independent times. Cell profile counting and measurement of depth of the circumvallate papilla were performed using ImageJ software. Statistical analysis (ANOVA with post hoc Tukey tests for Fig. 2F, 2G, or unpaired Student's t-test for Fig. 4D) was performed using GraphPad (Prism).

Organoid cultures: To generate taste organoids from adult wild-type and Trpm5-GFP mice, we followed the procedure we described previously (4). Briefly, cells were dissociated from circumvallate papilla tissue from at least three mice. After being filtered twice sequentially using 70- and 35- μm nylon mesh (Fisherbrand, Cat. # 22363548; Corning no. 352235), cells were plated directly onto low-attachment 24-well plates at a density of about 1×10^5 cells/well (Corning Ultra-Low Attachment Plates, Fisher Scientific, Cat. # 07-200-602), with 8% chilled Matrigel (Corning no. 356231) in 0.5 mL culture medium for each well. The same batch of cells was divided into two groups for comparison of the effect of R-spondin on taste cell generation.

The complete culture medium is composed of 20% DMEM/F12 medium (Life Technologies, Cat. # 11320033), 50% Wnt3a-conditioned medium (generated from a Wnt3a-producing cell line, gift from Dr. Hans Clevers, Hubrecht Institute, Netherlands,

under a materials transfer agreement; selected by 125 $\mu\text{g}/\text{mL}$ Zeocin), 20% R-spondin-conditioned medium (generated from an Rspo2 cell line, a gift of Dr. Jeffery Whitsett, University of Cincinnati, Cincinnati, OH, under a materials transfer agreement; selected by 600 $\mu\text{g}/\text{mL}$ Zeocin) or commercial recombinant Rspo2 (200 ng/mL, R&D, Cat. # 6946-RS-025), and 10% Noggin-conditioned medium (generated from a Noggin-producing cell line, selected by 400 $\mu\text{g}/\text{mL}$ Zeocin), supplemented with epidermal growth factor (50 ng/mL; Peprotech no. 315-09), N2 (1%; Life Technologies no. 17502-048), B27 (2% vol/vol; Life Technologies no. 17504044), and penicillin-streptomycin (1 \times ; ThermoFisher Scientific no. 15140122). R-spondin-free medium was the complete medium but with no added R-spondin-conditioned medium or commercial Rspo2. For the freshly dissociated single cells, Y-27632 (10 μM , Sigma Cat. # Y0503) was added to the medium to prevent dissociation-induced apoptosis. The medium was first changed after about 5 days of culturing and then every 2–3 days afterward.

Staining of organoids was performed as described previously. The anti-Car4 antibody (1:20; R&D, Cat. # AF2414, RRID: AB_2070332) or the endogenous GFP signal of Trpm5⁺ cells was used to visualize taste cells. Secondary antibody was donkey anti-goat Alexa Fluor 555 (1:500, Abcam, Cat. # 150130, RRID: AB_10894526).

Confocal images were compressed as z-stacks ($\sim 15 \mu\text{m}$) and acquired by a Leica SP2 confocal microscope. Scoring an organoid as positive for Car4 or Trpm5-GFP required at least one cell displaying a native taste-cell-like morphology, such as spindle-shaped, possessing a large spherical nucleus near the middle of the cell, and a fine process.

In situ hybridization: In situ hybridization was performed as described previously (5).

Briefly, euthanized mice were perfused with 4% paraformaldehyde; nodose-petrosal

ganglion complex and geniculate ganglia were then dissected out and embedded in O.C.T. Sections (8 μ m) were fixed with 4% paraformaldehyde, treated with diethylpyrocarbonate, prehybridized with salmon sperm DNA for 2 h at 58°C, and hybridized with fragmented antisense riboprobe(s) (~150 bases) overnight at 58°C after alkaline fragmentation. A digoxigenin-labeled antisense RNA probe was first generated using a clone including the complete coding sequence of Rspo2 (Horizon Discovery, Cat. # MMM1013-202805708) and fragmented under alkaline conditions. After hybridization, the sections were washed in 0.2 \times SSC at 58°C and blocked with 0.5% blocking reagent (Roche Diagnostics) in Tris-buffered saline. The sections were then incubated with alkaline phosphatase-conjugated anti-digoxigenin primary antibody (1:500, Roche Diagnostics, Cat. # 11207733910, RRID: AB_514500) for 1 h, followed by overnight incubation with chromogenic substrate 4-nitro blue tetrazolium chloride/5-bromo-4-chloro-3-indolyl-phosphate. Images were acquired with a Nikon Microphot microscope.

For double-label fluorescence in situ hybridization, fluorescein-labeled Rspo2 probes and digoxigenin-labeled Phox2b or P2X2 (which is encoded by P2rx2) probes were sequentially detected as follows. Phox2b antisense probes were generated using a construct subcloned from a full-length clone (Horizon Discovery, Cat. # MMM1013-202797591) (~2.1 kb), and P2X2 antisense probes were generated using a clone containing 1-1568 bp of BC106964. After hybridization, washing, and blocking, sections were incubated with a biotin-conjugated anti-fluorescein antibody (1:500, Vector Laboratories, Cat. # BA-0601; RRID: AB_2336069) for 1 h, incubated with an avidin-biotin complex (Vector, VECTASTAIN Elite ABC Kit) for 30 min, incubated with TSA (tyramide signal amplification)-plus biotin solution (1:50, PerkinElmer, TSA Plus Biotin

Kit) for 10 min, and then incubated with an Alexa488-conjugated streptavidin (1:500, Thermo Fisher Scientific) for 30 min. After treatment with 3% H₂O₂ in PBS for 60 min to inactivate horseradish peroxidase (HRP), sections were incubated with an HRP-conjugated anti-digoxigenin antibody (1:500, Roche, Cat. # 11207733910; RRID: AB_514500) for 1 h and incubated with TSA-plus Cyanine 3 solution (1:50, PerkinElmer, TSA Plus Cyanine 3 System) for 10 min. The fluorescent images were acquired using a confocal microscope (Leica SPE) with a pinhole size of 1.0 Airy unit.

qPCR analysis: Gustatory ganglia were harvested from adult mice. RNA was extracted using the PureLink™ RNA Micro Kit (ThermoFisher, 12183-016) according to the manufacturer's directions and treated with DNase I to remove genomic DNA. cDNA was synthesized using SuperScript™ IV VILO™ Master Mix (Invitrogen, 11766500), and qPCR was performed using Fast SYBR Green Master Mix Kit (Applied Biosystems, 4385612). Melting temperature was used as quality control for qPCR. Gapdh was used as control to normalize the transcripts expression levels of target genes. The relative gene expression was calculated as $2^{- (CT_{\text{Target}} - CT_{\text{Gapdh}})}$. RNA without reverse transcriptase showed a negligible level of amplification.

The prime sets included Rspo1 (forward: GTCAACGGTTGCCTCAAGTG, reverse: TGCGGGCATCAAAGTATCCA, length: 115 bp), Rspo2 (forward: CTTCCAGGAGCCCGTCATTT, reverse: CGCTTATTGCGTCTCCATCG, length: 155 bp), Rspo3 (forward: CATGTGGCTTCAAAGGGGG, reverse: GTTCTTGTCTCGCTGGTTGG, length: 100 bp), Rspo4 (forward: CACGGGCTGTGTCATATGCT, reverse: CACTTGCCGTACTGACGGAT, length: 102

bp), Phox2b (forward: AA ACTCTTCACCGACCACGG, reverse:
GTCAGGGTAGTGCGTCTCAG, length: 123 bp), and Gapdh (forward:
TTGCAGTGGCAAAGTGGAGA, reverse: GTCTCGCTCCTGGAAGATGG, length:
175 bp).

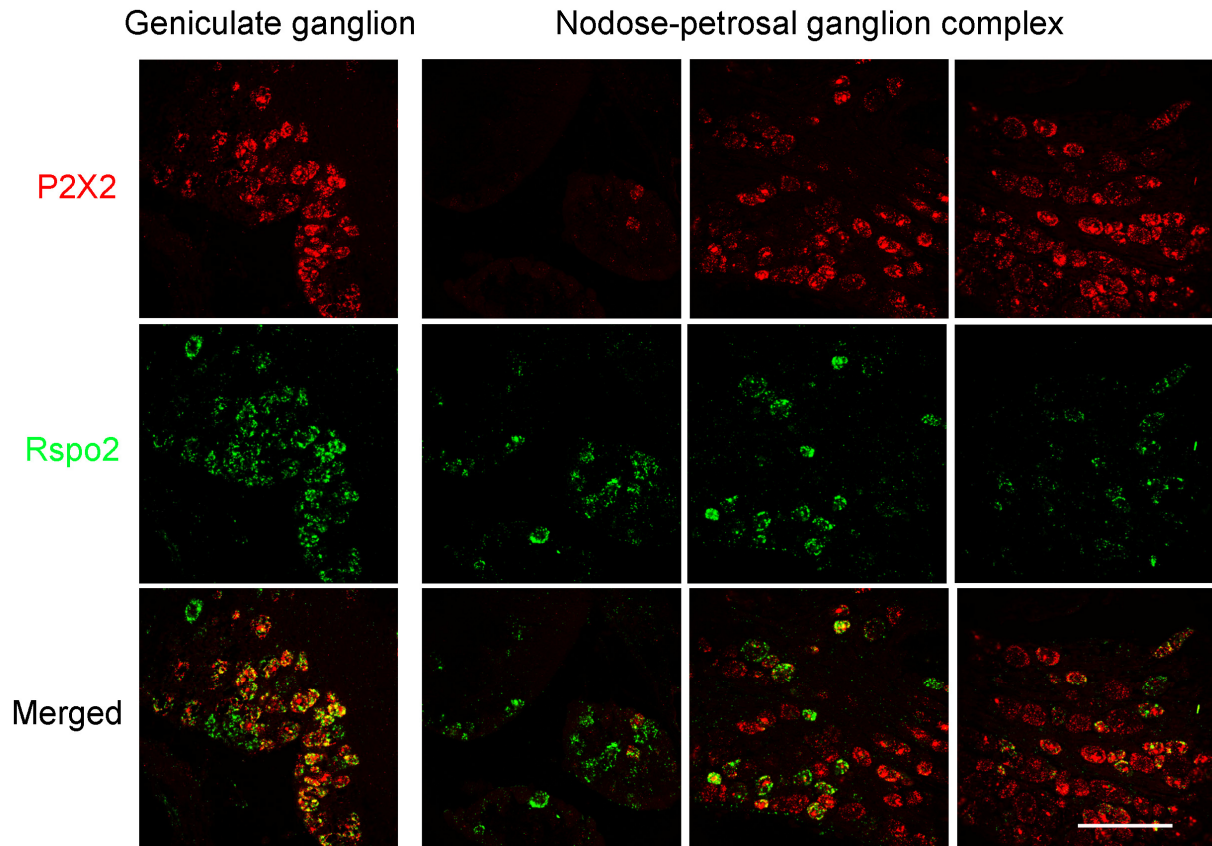


Fig. S2. Co-localization of *Rspo2* and *P2rx2* (encoding P2X2) in the geniculate ganglion and the nodose-petrosal ganglion complex (NPG). Representative images of dual *in situ* hybridization with *P2rx2* (P2X2) and *Rspo2* antisense probes show the co-localization of *Rspo2* (green) and *P2rx2* (P2X2, red) in a large set of neurons in the geniculate ganglion and NPG (three adjacent fluorescent images were taken to show the whole structure of the NPG). Scale bar: 100 μ m.

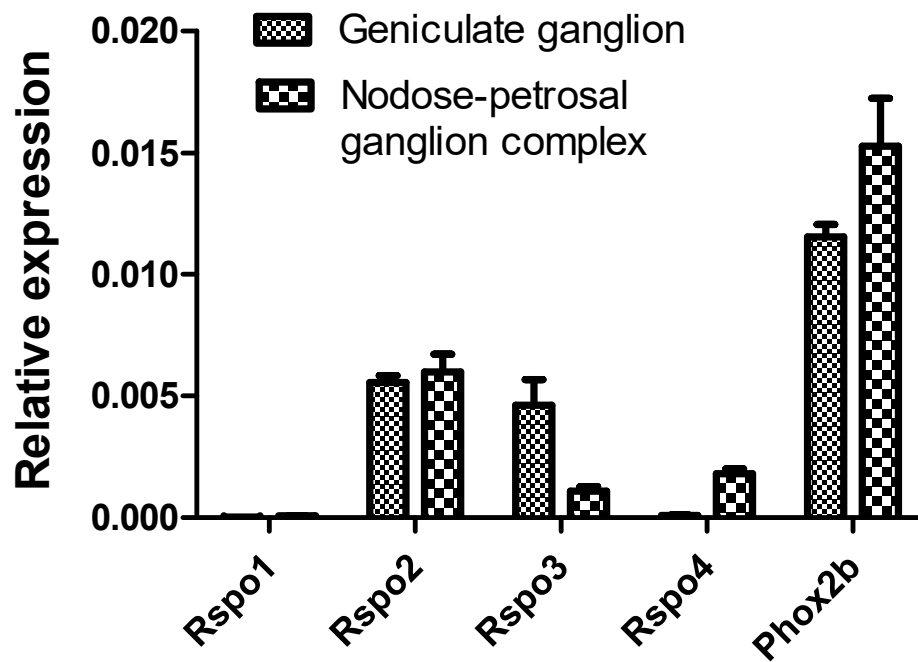


Fig. S3. qRT-PCR analysis of the expression of R-spondins in gustatory ganglia. Expressions of *Rspo2* and other R-spondin genes (*Rspo1*, *Rspo3*, *Rspo4*) and *Phox2b* in the geniculate ganglion and nodose-petrosal ganglion complex were determined by real-time quantitative PCR. The expression levels of these genes were normalized to that of *Gapdh*. Data (mean \pm SEM) are biological replicates (n = 3 or 4).

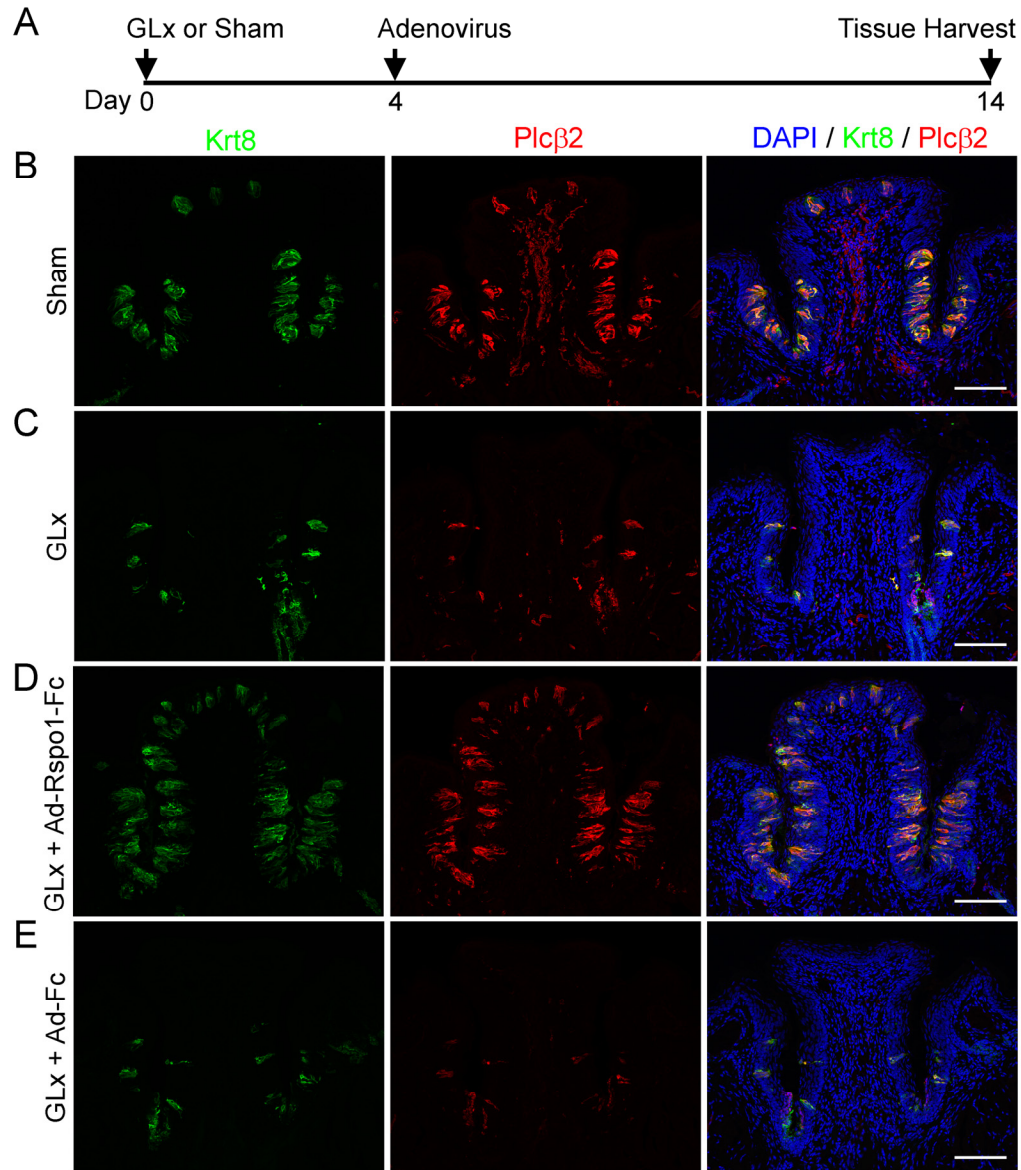


Fig. S4. Taste cells and taste buds are present in GLx mice receiving Ad-Rspo1-Fc (see also Fig. 2). **A)** Schematic of experiment design. **B-E)** Representative confocal images of immunostaining of circumvallate papilla sections with antibodies against Krt8 (*left panels*) and Plc β 2 (*middle panels*). *Right panels*: Merged images, counterstained with DAPI. **B)** Sham-operated mice, showing typical Krt8⁺ and Plc β 2⁺ cells in taste buds. **C)** GLx mice. Note no or fewer Krt8⁺ and Plc β 2⁺ cells in the circumvallate papilla. Krt8⁺ cells are noted in the collecting duct outside the circumvallate papilla. **D)** GLx mice infected with Ad-Rspo1-Fc. Numerous Krt8⁺ and Plc β 2⁺ taste cells are present in the circumvallate papilla despite GLx. **E)** GLx mice infected with control adenovirus (Ad-Fc). No or few Krt8⁺ and Plc β 2⁺ cells are present in the circumvallate papilla. Images were acquired using the same settings. Four mice were used for each experiment, except for control adenovirus Ad-Fc infection (three mice). Scale bars: 100 μ m.



Fig. S5. Representative images of the entire small intestine from four different experimental groups: Sham, GLx, GLx + Ad-Rspo1-Fc, and GLx + Ad-Fc. Note hypertrophy of the small intestine in mice infected with Ad-Rspo1-Fc but not in other mice.

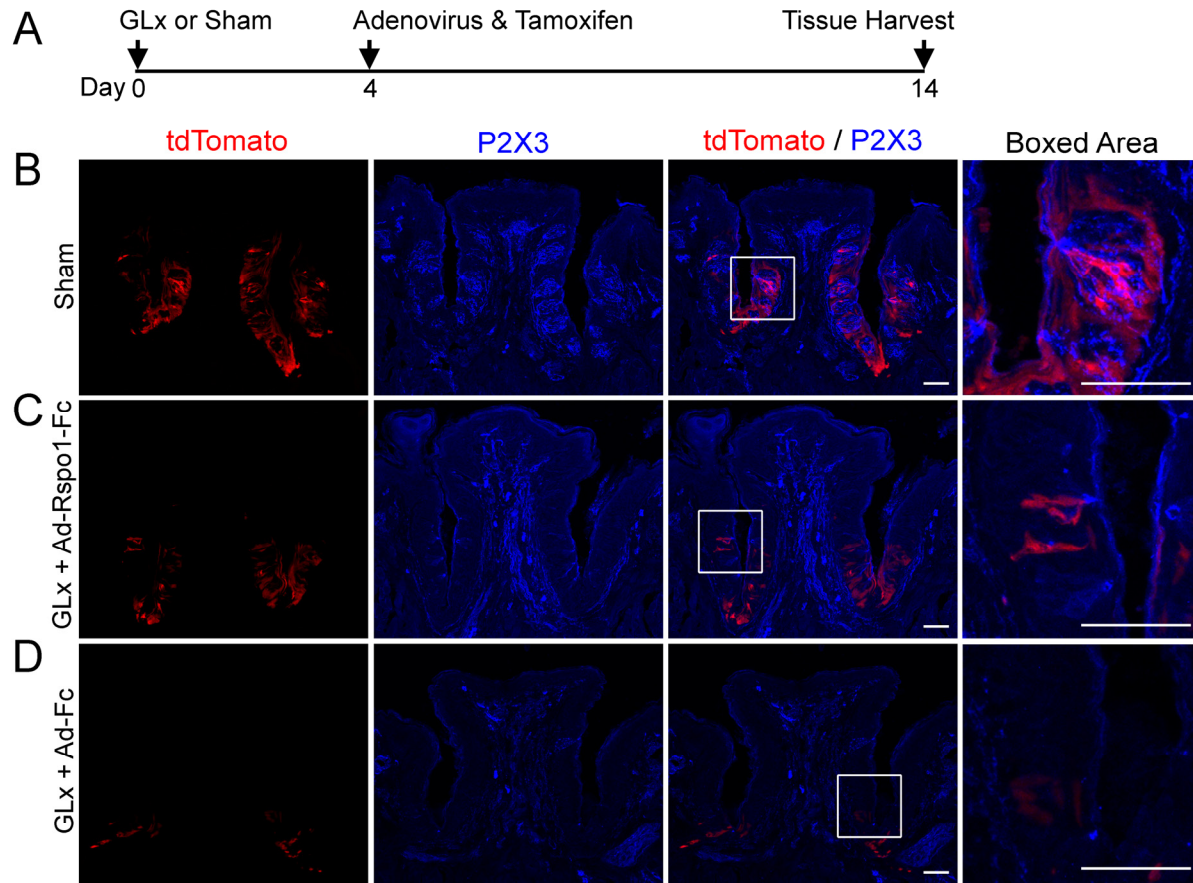


Fig. S6. $Lgr5^+$ cells contribute to taste bud cell generation in GLx mice infected Ad-Rspo1-Fc (see also Fig. 3). **A**) Schematic of experimental design. Adenoviral infection and tamoxifen induction were performed at day 4 after GLx. Tissues were collected at day 14 after GLx. **B-D**) Lineage tracing of $Lgr5^+$ cells in circumvallate papilla sections from $Lgr5^{EGFP-IRES-CreERT2/+}; Rosa26^{tdTomato}$ mice using tdTomato (red; *left panels*). Sections were costained with anti-P2X3 antibody (blue; *second panels*) to show the presence of P2X3-positive nerve terminals in taste buds. The boxed areas of the merged images (*third panels*) highlight taste buds containing both P2X3⁺ nerve terminal and tdTomato⁺ cells (*right panels*). **B**) Sham-operated mice (10 days after tamoxifen induction). Many tdTomato⁺ cells are present within taste buds and outside taste buds in the circumvallate papilla, consistent with results shown in Fig. 2. **C**) GLx mice infected with Ad-Rspo1-Fc. The boxed area shows presence of tdTomato⁺ taste cells (based on morphology) but absence of P2X3⁺ nerve terminal in the epithelial layer. **D**) GLx mice infected with control adenovirus (Ad-Fc). The boxed area shows the presence of tdTomato⁺ cells (based on morphology) but absence of P2X3⁺ nerve terminal in the epithelium layer. A few tdTomato⁺ cells are visible in the trench area of the circumvallate papilla (boxed area), but they do not show a typical taste-cell morphology. Images were acquired using the same settings. Each experiment was performed using two mice, except sham-operated (three mice). Scale bars: 50 μ m.

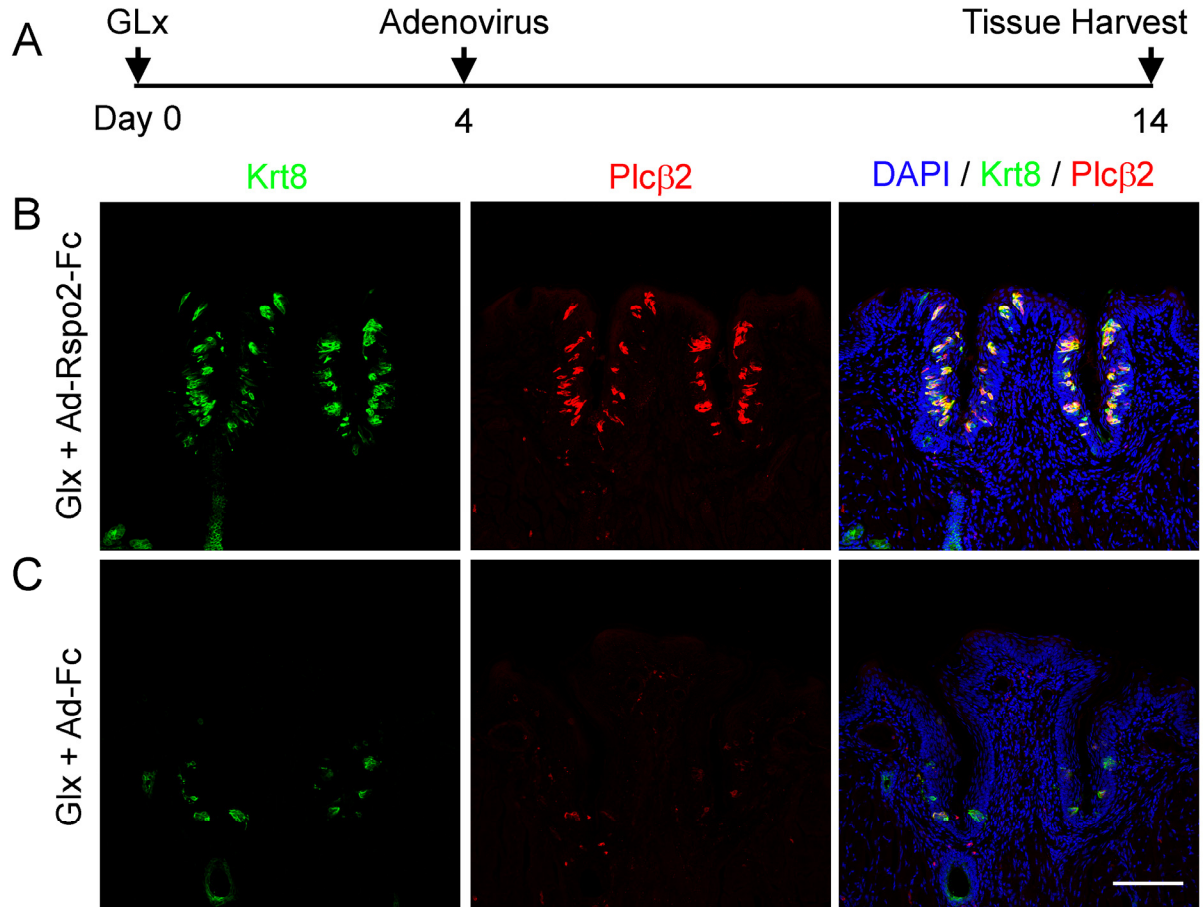


Fig. S7. Taste cells and taste buds are present in GLx mice receiving Ad-Rspo2-Fc (see also Fig. 4). **A)** Schematic of experiment design. **B, C)** Representative confocal images of immunostaining of circumvallate papilla sections with antibodies against Krt8 (*left panels*) and Plcβ2 (*middle panels*). *Right panels*: Merged images, counterstained with DAPI. **B)** GLx mice infected with Ad-Rspo2-Fc (n = 4). Numerous Krt8⁺ and Plcβ2⁺ taste cells are present in the circumvallate papilla despite GLx. **C)** GLx mice infected with control adenovirus (Ad-Fc, n = 3). No or few Krt8⁺ and Plcβ2⁺ cells are present in the circumvallate papilla. Images were acquired using the same settings. Scale bar: 100 μm.

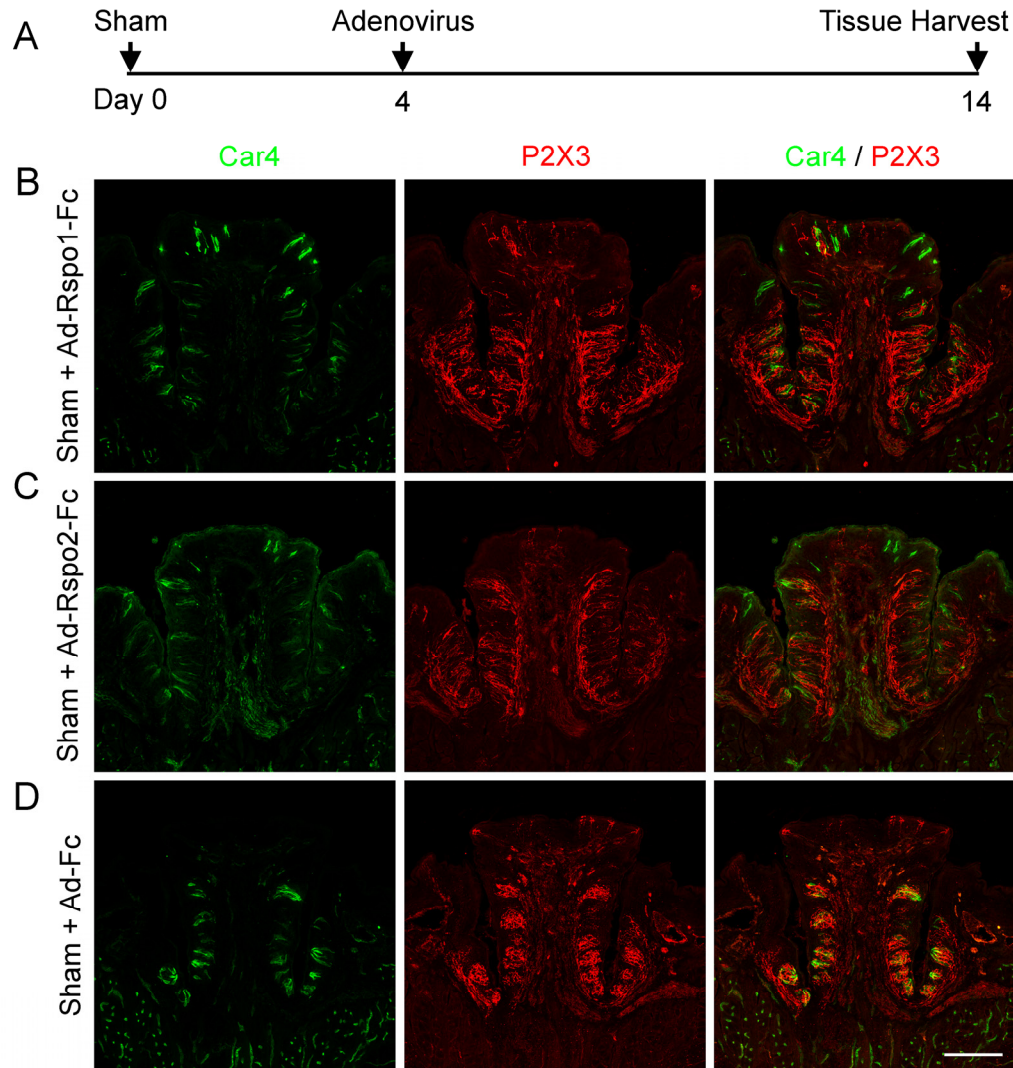


Fig. S8. Characterization of the circumvallate papilla of sham-operated mice receiving Ad-Rspo1-Fc (B), Ad-Rspo2-Fc (C), or Ad-Fc (D) using anti-Car4 and anti-P2X3 antibodies. A) Schematic of experiment design. B-D) Representative confocal images of immunostaining of circumvallate papilla sections with antibodies against Car4 (*left panels*) and P2X3 (*middle panels*). Right panels are merged images. The pattern of Car4⁺ cells in mice infected with Ad-Rspo1-Fc (3×10^8 pfu, $n = 2$) (B) or Ad-Rspo2-Fc (1×10^9 pfu, $n = 4$; C) is similar to that in GLx mice infected with Ad-Rspo1-Fc (Fig. 2D) or Ad-Rspo2-Fc (Fig. 4B). Ectopically expressed differentiated Car4⁺ cells are visible in the dorsal surface of the circumvallae papilla. The pattern of Car4⁺ cells in mice infected with Ad-Fc (1×10^9 pfu, $n = 3$; D) is similar to that in sham-operated mice without virus infection (Fig. 2B). Strong P2X3-immunoreactive signals staining nerve terminals were detected in taste buds (B-D). P2X3⁺ terminals appear to be less organized in mice treated with Ad-Rspo1-Fc or Ad-Rspo2-Fc (B, C, red) compared with mice treated with Ad-Fc (D, red). Images were acquired using the same settings. Scale bar: 100 μ m.

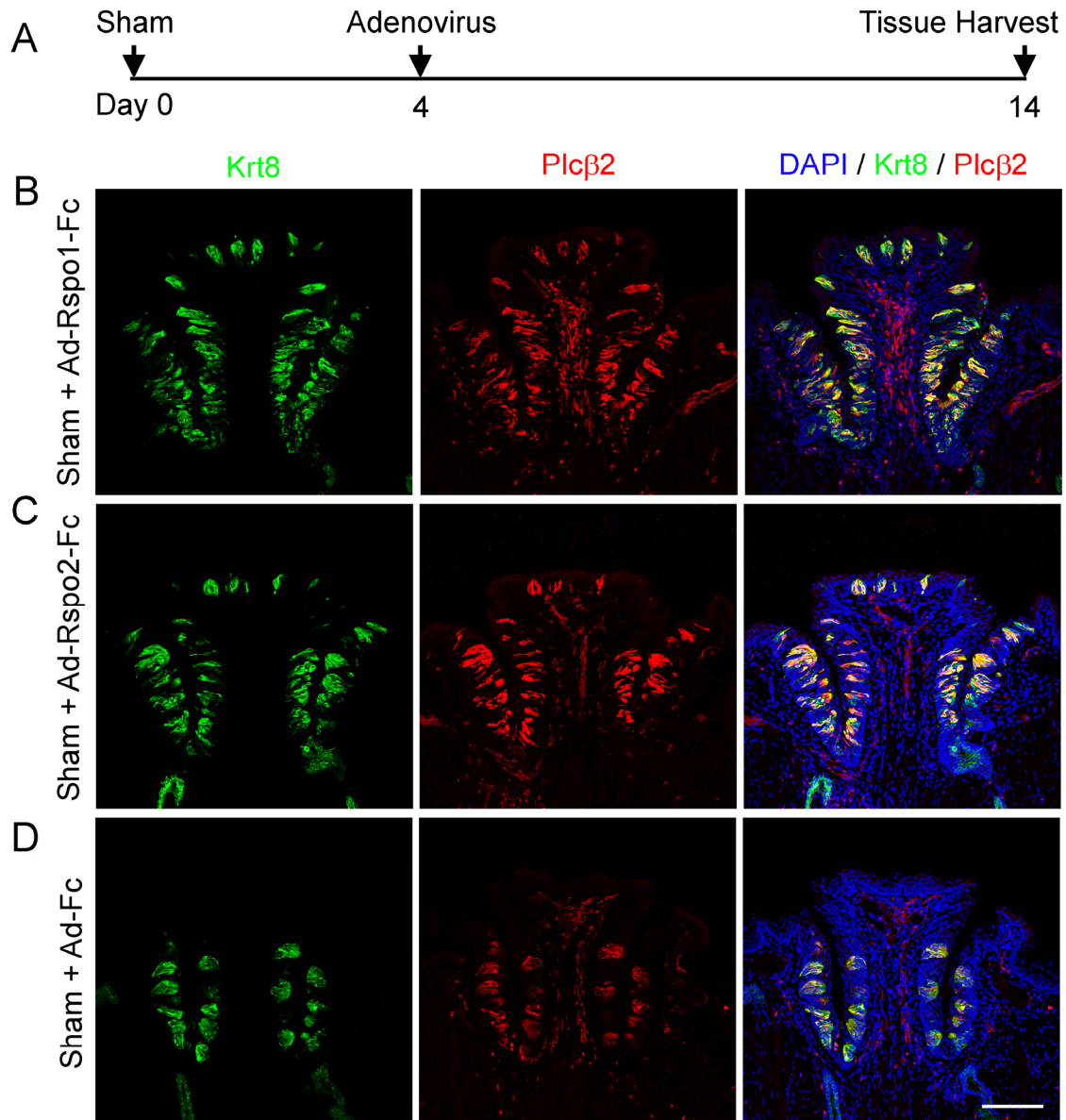


Fig. S9. Characterization of the circumvallate papilla of sham-operated mice receiving Ad-Rspo1-Fc (B), Ad-Rspo2-Fc (C) and Ad-Fc (D) using anti-Krt8 and anti-Plcβ2 antibodies (see also Fig. S8). **A**) Schematic of experiment design. **B-D**) Representative confocal images of immunostaining of circumvallate papilla sections with antibodies against Krt8 (*left panels*) and Plcβ2 (*middle panels*). Right panels are merged images (Krt8/ Plcβ2). The pattern of Plcβ2⁺ (red) and Krt8⁺ (green) cells in mice infected with Ad-Rspo1-Fc (n = 2) or Ad-Rspo2-Fc (n = 4) is similar to that in GLx mice infected with Ad-Rspo1-Fc (Fig. S4D) or Ad-Rspo2-Fc (Fig. S7B). The pattern of Plcβ2⁺ (red) and Krt8⁺ (green) cells in mice infected with Ad-Fc (n = 3) is similar to that in sham-operated mice without virus infection (**Fig. S4B**). Scale bar: 100 μm

SI References:

1. Takeda N, *et al.* (2013) Lgr5 Identifies Progenitor Cells Capable of Taste Bud Regeneration after Injury. *PLoS One* 8(6):e66314.
2. Ren W, *et al.* (2014) Single Lgr5- or Lgr6-expressing taste stem/progenitor cells generate taste bud cells ex vivo. *Proc Natl Acad Sci U S A* 111(46):16401-16406.
3. Yee KK, *et al.* (2013) Lgr5-EGFP marks taste bud stem/progenitor cells in posterior tongue. *Stem Cells* 31(5):992-1000.
4. Ren W, *et al.* (2017) Transcriptome analyses of taste organoids reveal multiple pathways involved in taste cell generation. *Sci Rep* 7(1):4004.
5. Lei W, *et al.* (2018) Activation of intestinal tuft cell-expressed *Sucnr1* triggers type 2 immunity in the mouse small intestine. *Proc Natl Acad Sci U S A* 115(21):5552-5557.
6. Dvoryanchikov G, *et al.* (2017) Transcriptomes and neurotransmitter profiles of classes of gustatory and somatosensory neurons in the geniculate ganglion. *Nat Commun* 8(1):760.